

Deep Neural Network Based Accelerated Failure Time Models using Rank Loss.

Gwangsu Kim^a, Sangwook Kang^{b,c,*}

^a*School of Electrical Engineering, KAIST, Daehak-ro, 291 Yuseong-gu, Daejeon, Republic of Korea*

^b*Department of Applied Statistics, Yonsei University, 50 Yonsei-ro, Seodaemun-gu, Seoul, Republic of Korea*

^c*Department of Statistics and Data Science, Yonsei University, 50 Yonsei-ro, Seodaemun-gu, Seoul, Republic of Korea*

Abstract

An accelerated failure time (AFT) model assumes a log-linear relationship between failure times and a set of covariates. In contrast to other popular survival models that work on hazard functions, the effects of covariates are directly on failure times, whose interpretation is intuitive. The semiparametric AFT model that does not specify the error distribution is flexible and robust to departures from the distributional assumption. Owing to the desirable features, this class of models has been considered as a promising alternative to the popular Cox model in the analysis of censored failure time data. However, in these AFT models, a linear predictor for the mean is typically assumed. Little research has addressed the nonlinearity of predictors when modeling the mean. Deep neural networks (DNNs) have received a focal attention over the past decades and have achieved remarkable success in a variety of fields. DNNs have a number of notable advantages and have been shown to be particularly useful in addressing the nonlinearity. By taking advantage of this, we propose to apply DNNs in fitting AFT models using a Gehan-type loss, combined with a sub-sampling technique. Finite sample properties of the proposed DNN and rank based AFT model (DeepR-AFT) are investigated via an extensive stimulation study. DeepR-AFT shows a superior performance over its parametric or semiparametric counterparts when the predictor is nonlinear. For linear predictors, DeepR-AFT performs better when the dimensions of covariates are large. The proposed DeepR-AFT is illustrated using two real datasets, which demonstrates its superiority.

Keywords: Deep neural network, Nonlinearity, Gehan loss, Survival analysis, C-index, Semiparametric accelerated failure time model

1. Introduction

For a regression modeling of failure times, an accelerated failure time (AFT) assumption is often postulated. The AFT model relates a log-transformed failure time to a linear combination of regression coefficients and a set of covariates added by a zero-mean random error term. The AFT model can be either parametric or semiparametric, depending on whether the distribution of the error term is assumed to be parametric or left unspecified, respectively. The latter shares the flexibility of the well-known Cox proportional hazards model (Cox, 1972) and has therefore been viewed as a viable alternative. Parametric AFT models can be inferred using the usual maximum likelihood method. For semiparametric AFT models, rank-based methods have been popular (Prentice, 1978; Jin et al., 2003, 2006; Johnson and Strawderman, 2009) among others including the least-squares estimation (Buckley and James, 1979; Stute, 1993; Jin et al., 2006). The theoretical properties of the rank-based estimators have been rigorously investigated and well established (Tsiatis, 1990; Ying, 1993; Fygenon and Ritov, 1994). Popular statistical software such as R implements some of these methods, which have made fitting censored survival data based on AFT models routine analysis. For example, maximum likelihood estimators for regression coefficients in parametric AFT models can be obtained by the `survreg` function in the `survival` package in R (Therneau, 2020). Rank-based estimators for semiparametric AFT models are implemented in the `aftgee` package in R (Chiou et al., 2014).

*Corresponding author

Email addresses: `s88012@kaist.ac.kr` (Gwangsu Kim), `kanggi1@yonsei.ac.kr` (Sangwook Kang)

The aforementioned development in AFT modeling approach is mostly based on the assumption that the effects of covariates are linear or, more generally, parametric. This simplified depiction of the covariate effects has several benefits including a direct summary of the covariate effect that allows for a straightforward and intuitive interpretation of the covariate effect. Meanwhile, when the underlying relationship between covariates and failure times is complex and nonlinear, this linear modeling approach may be too restrictive and lead to biased results since it does not properly reflect the true underlying relationship. This could be even more problematic when a prediction of survival times is of main interest, as is the case in many clinical and biological studies. In this situation, a more accurate prediction is anticipated by imposing a nonlinear relationship that nonparametrically models the mean function part. Some efforts have been made to allow a nonparametric modeling of AFT models under the framework of the smoothing spline with penalization (Leng and Ma, 2007). Although interaction terms can also be handled in this approach, low-order terms are typically considered to control the model complexity (Huang et al., 2000; Leng and Ma, 2007). Deep neural networks (DNNs) have been shown to be particularly successful in addressing nonlinearity and interactions (Katzman et al., 2018; Kvamme et al., 2019). In this manuscript, we propose a DNN-based model and algorithm, referred to as DeepR-AFT.

Considering the recent success of DNNs, applying DNNs to AFT models can be an effective method for addressing the nonlinearity. By virtue of their model complexity and optimization techniques, DNNs have proven successful in prediction in survival analysis, as reported in a variety of fields, including medicine (He, 2020; Chattopadhyay et al., 2020; Lundervold and Lundervold, 2019). DNNs’ capacity to model and predict nonparametric functions with large dimensional variables and their interactions is one of their many prominent advantages. DNNs are recognized to have a strong representation power and have been adapted to numerous tasks of natural language processing and reinforcement learning. Recent efforts have been made to use DNNs in the context of survival analysis, which commonly use Cox or discretized hazard models (Katzman et al., 2018; Lee et al., 2018; Chapfuwa et al., 2018; Kvamme et al., 2019; Zhao and Feng, 2020; Rava and Bradic, 2020). A DNN-cooperative meta-learning algorithm was proposed more recently (Qiu et al., 2020). It demonstrates a remarkable performance in the use of small datasets through “learn to learn”. With the exception of Kvamme et al. (2019), who provided the approach that uses mini-batches in DNNs, most previous works based on partial-likelihood structure use a full batch in the stochastic gradient (SGD) algorithm. This is mainly due to the existence of risk sets, a stochastic property in the popular partial-likelihood. Scalability becomes an issue when using DNNs because a mini-batch requires the full data for a specific case. In contrast, the Gehan loss in AFT models takes into account all pairs, not depending on risk sets. With this feature, an application of the mini-batch algorithm becomes easily feasible and, thus, leads to achieve the scalability.

computational order is quadratic in sample size. We propose a sub-sampling procedure that can reduce the computational order to linear in the scale of the sample size. Since the resulting sample can be regarded as a random sample from all possible pairs, the stochastic descent algorithm (SGD) in mini-batches can be readily applied. This scalability has rarely been addressed in the existing literature using DNNs in survival analysis.

Limited research has been conducted on the use of DNNs in AFT models. The deepAFT, proposed by Chen and Norman (2019), uses the DNN in the semiparametric AFT model, primarily via Buckley-James or inverse-probability-censoring-weight type losses. Surprisingly, the Gehan loss, a popular loss for semiparametric AFT models, has little been considered to use DNNs in the published literature. In addition, the deep extended hazard model (deep EH; Zhong et al., 2021) was proposed, which considered general models including the AFT model as a special case. The loss function is therefore not specific to the AFT model. When AFT models are considered, it can diminish the accuracy of predictions in comparison to the Gehan loss. In turn, we propose to study a more specific DNN suitable for an AFT model using the Gehan loss, popular in the semi-parametric AFT models. Given that the computational order is quadratic in sample size, a direct evaluation of the Gehan loss could be computationally intensive. In order to alleviate this computational burden, we propose a sub-sampling of pairs that can reduce the computational order to linear in the sample size.

The rest of the paper is organized as follows. In Section 2, a summary of existing approaches for fitting AFT models is provided. The proposed DNN modeling approach for nonlinear AFT models is introduced in Section 3. Section 4 presents the results of the extensive simulation experiments conducted under various aspects including different mean functions, bias and variance trade-offs, and large dimensional covariates.

We illustrate our proposed DNN approach using two real datasets in Section 5. In Section 6, we conclude with a summary and a discussion of possible future work directions.

2. Conventional parametric and semiparametric AFT modeling

2.1. Setup and model

Let T denote the potential failure time. T may not be observable due to right censoring. Let C denote the potential censoring time. Then, the observed time is $Y = \min(T, C)$ and $\Delta = \mathbb{I}(T \leq C)$ denote the indicator for failure where the $\mathbb{I}(\cdot)$ is an indicator function. We assume that T and C are conditionally independent given \mathbf{x} where \mathbf{x} is a p -dimensional vector of covariates. Data for n subjects can be represented by independent and identically distributed (*i.i.d*) copies of (Y, Δ, \mathbf{x}) , $(Y_i, \Delta_i, \mathbf{x}_i)$, $i = 1, \dots, n$. We impose an AFT model for T_i given \mathbf{x}_i where

$$\log T_i = f(\mathbf{x}_i) + \epsilon_i, \quad i = 1, \dots, n. \quad (1)$$

Here, $f(\mathbf{x}_i)$ can be set to a linear or nonlinear function and ϵ_i is a zero-mean random error term with a finite variance.

2.2. Inference for parametric AFT models

When the distribution of ϵ_i is known, it is referred to as a parametric AFT model. We typically consider the linear case for the mean function, i.e., $f(\mathbf{x}_i) = \mathbf{x}_i^\top \boldsymbol{\beta}$. Parametric AFT models are often represented by $\log T_i = \mathbf{x}_i^\top \boldsymbol{\beta} + \sigma \epsilon_i$ where σ is a scale parameter. For inferences, likelihood-based approaches have typically been employed. A likelihood function under the setup described in Section 2.1 is given as

$$L(\boldsymbol{\theta}) = \prod_{i=1}^n f_T(y_i; \boldsymbol{\theta})^{\Delta_i} S_T(y_i; \boldsymbol{\theta})^{1-\Delta_i}$$

where $f_T(\cdot; \boldsymbol{\theta})$ and $S_T(\cdot; \boldsymbol{\theta})$ are the probability density and survival functions for T , respectively, and $\boldsymbol{\theta} = (\boldsymbol{\beta}^\top, \sigma)^\top$. The estimator of $\boldsymbol{\theta}$ is then defined as the maximizer of $L(\boldsymbol{\theta})$ and termed as the maximum likelihood estimator (MLE) of $\boldsymbol{\theta}$. Its large sample properties such as consistency and asymptotic normality are well established under certain regularity conditions. For more detailed discussion, see Klein and Moeschberger (2006) or Collett (2015).

2.3. Rank-based inference for semiparametric AFT models

Unlike parametric AFT models, in semiparametric AFT models, the distribution of ϵ_i is left unspecified. We still consider $f(\mathbf{x}_i) = \mathbf{x}_i^\top \boldsymbol{\beta}$, linear relationship for the mean function. Rank-based estimators for semiparametric AFT models are based on weighted estimating functions constructed using the ranks of the censored residuals, $e_i(\boldsymbol{\beta}) = \log Y_i - \mathbf{x}_i^\top \boldsymbol{\beta}$, $i = 1, \dots, n$. Specifically, estimating functions with the Gehan-type weight are (Prentice, 1978; Jin et al., 2003)

$$U_G(\boldsymbol{\beta}) = \sum_{i=1}^n \sum_{j=1}^n \Delta_i (\mathbf{x}_i - \mathbf{x}_j) \mathbb{I}\{e_j(\boldsymbol{\beta}) \geq e_i(\boldsymbol{\beta})\}. \quad (2)$$

The rank-based estimator for $\boldsymbol{\beta}$ is then defined as the solution to $U_G(\boldsymbol{\beta}) = 0$. Note that (2) is a gradient of the convex function

$$\sum_{i=1}^n \sum_{j=1}^n \Delta_i [e_i(\boldsymbol{\beta}) - e_j(\boldsymbol{\beta})]^{-}, \quad (3)$$

where $[a]^{-}$ denotes $|\min(a, 0)|$. Therefore, the rank-based estimator for $\boldsymbol{\beta}$ can be equivalently obtained by minimizing (3). The resulting estimator for $\boldsymbol{\beta}$ were shown to be consistent and asymptotically normally

distributed (Ritov, 1990; Ying, 1993; Jin et al., 2003). An induced smoothed version of (2) is a more recently proposed variant of rank-based estimators and has the following form:

$$\tilde{U}_G(\boldsymbol{\beta}) = \sum_{i=1}^n \sum_{j=1}^n \Delta_i(\mathbf{x}_i - \mathbf{x}_j) \Phi \left\{ \frac{e_j(\boldsymbol{\beta}) - e_i(\boldsymbol{\beta})}{r_{ij}} \right\},$$

where $r_{ij} = n^{-1}(\mathbf{x}_i - \mathbf{x}_j)^\top (\mathbf{x}_i - \mathbf{x}_j)$. This modified rank-based estimator is shown to be asymptotically equivalent to the estimator solving $U_G(\boldsymbol{\beta}) = 0$ or minimizing (3) while providing a computationally more efficient variance estimate (Brown and Wang, 2007; Johnson and Strawderman, 2009; Chiou et al., 2015).

3. DNN modeling for f in the nonlinear-nonparametric AFT model

3.1. Nonlinear-nonparametric AFT model

When f is nonlinear and the error distribution is not specified, it is referred to as a nonlinear-nonparametric AFT model. Here, we adopt a parameter \mathbf{w} to model the nonlinear f without transforming covariates. For example, spline basis functions can be used for $f_{\mathbf{w}}$ to model the nonlinearity. We propose to model f using DNNs to effectively address the possible nonlinearity with a complex structure such as interactions. To infer an nonlinear-nonparametric AFT model, we also propose to use the following Gehan loss:

$$\sum_{i=1}^n \sum_{j=1}^n \Delta_i [e_i(\mathbf{w}) - e_j(\mathbf{w})]^{-}, \quad (4)$$

where $e_i(\mathbf{w}) = \log Y_i - f_{\mathbf{w}}(\mathbf{x}_i)$, $i = 1, \dots, n$.

3.2. DeepR-AFT

The loss function (4) is designed to extend the mean modeling from $\mathbf{x}^\top \boldsymbol{\beta}$ to nonlinear-nonparametric $f_{\mathbf{w}}(\mathbf{x})$. In this extension, we propose to use a DNN to estimate the nonlinear f . By using multiple layers with nonlinear activation, such as rectified linear unit (ReLU), we can capture the nonlinear relationship between the covariate and the mean of log-transformed failure time in an AFT model. The DNN can provide the model capacity for the nonlinear f . The landscape demonstrating the proposed network is drawn in Figure 1. Let $\sigma(\cdot)$ and \mathbf{W}_l be an activation vector function, weight matrix for the l^{th} layer, respectively. Then $f(\mathbf{x})$ is modeled by $f_{\mathbf{w}}$ where

$$f_{\mathbf{w}}(\mathbf{x}) = \sigma_L(\mathbf{W}_L(\sigma(\mathbf{W}_{L-1}(\cdots \sigma(\mathbf{W}_l(\cdots \sigma(\mathbf{W}_1 \mathbf{x}) \cdots)) \cdots))).$$

Here, $\sigma(\cdot)$ is a vector function having the identical functions on the element of input vector, and the activation function for the last layer, $\sigma_L(\cdot)$ is a linear function the output of which is one-dimensional real number. Temporarily, we drop the bias terms (intercepts) for notational simplicity, which can be easily added in practice.

The proposed network uses the pair-wise loss and weight-sharing for $f_{\mathbf{w}}(\mathbf{x}_1)$ and $f_{\mathbf{w}}(\mathbf{x}_2)$. Details on hyperparameters, including the number of layers, are as follows. In the proposed networks, three layers having ReLU as the activation function is adopted, and the last layer has a linear activation for regression. There are 128, 32, and 16 nodes for three layers, respectively. We model f with the same parameters by weight sharing. Then, the loss function is the Gehan loss defined in the equation (2), and a SGD algorithm is used with a mini-batch. We construct a matched dataset by a sub-sampling (see Section 3.3). After that, we select random samples of size b from the matched dataset where b is the size of the mini-batch. Detailed learning setups for DNN, including the batch size, epochs, and optimizers, are deferred to Appendix A. We call our proposed DNN and rank loss based AFT model as DeepR-AFT.

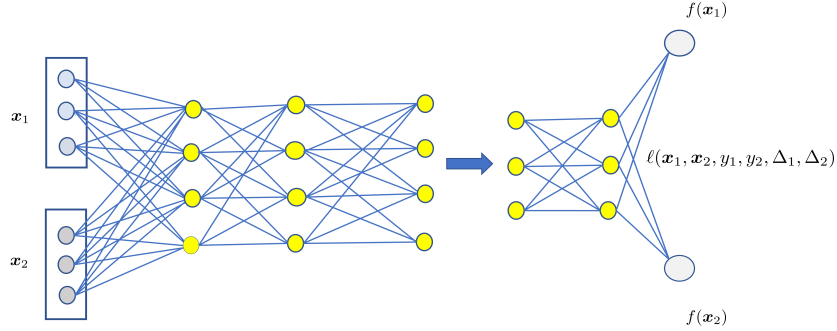


Figure 1: Architecture for DeepR-AFT. The outputs $f(\mathbf{x}_1)$ and $f(\mathbf{x}_2)$ share the parameters, and $\ell(f(\mathbf{x}_1), f(\mathbf{x}_2), Y_1, Y_2, \Delta_1, \Delta_2) = \mathbb{I}(\Delta_1 = 1)[\log Y_1 - \log Y_2 - f(\mathbf{x}_1) + f(\mathbf{x}_2)]^-$.

3.3. Sub-sampling pairs with DeepR-AFT

The Gehan loss (4) requires pair-wise evaluations of all pairs from the n samples. The resulting computational order is thus $O(n^2)$. One approach to reduce this computational complexity is to sample pairs instead of evaluating all pairs. This sub-sampling idea has been recently explored in the context of completely observed massive data with large n (Ma et al., 2014; Wang et al., 2018; Wang and Ma, 2021). For censored survival data, literature is rather limited. Zuo et al. (2021) and Keret and Gorfine (2020) developed sub-sampling approaches under an additive hazards model and Cox proportional hazard model with rare events, respectively. In this paper, we consider a similar sub-sampling idea. We propose a pair-wise sampling and learning method in DNNs. Since the Gehan loss is formed by constructing all possible pairs between all residuals and residuals concerning non-censored failure times, we propose a sub-sampling approach from all pairs in Gehan loss, i.e., sampling from $\{(Y_i, Y_j)\}_{\delta_i=1, j \neq i}$. Specifically, for each non-censored failure time Y_i , we sample s pairs from $n - 1$ possible pairs. Finally, we obtain sub-samples from all possible pairs whose less than $n \times s$. For example, we can use $s = 5$ or 10 when $n = 1000$ and 5000 , respectively.

The proposed sub-sampling procedure has the following merits. First, it reduces the computational order from quadratic to linear in the scale of the sample size. Second, this sub-sampling procedure still works for the SGD since the resulting sample can be regarded as a random sample from all possible pairs in Gehan loss. The mini-batches for the SGD algorithm can be obtained through the b samples (mini-batch) from sub-sampled pairs. We can use the following loss for each mini-batch with size b :

$$\sum_{i=1}^k \sum_{j=1}^{r_k} \Delta_i [e_i(\mathbf{w}) - e_j(\mathbf{w})]^- , \quad (5)$$

where $\sum_{i=1}^k r_k = b$. Here, the pairs in the equation (5) is randomly obtained from sub-sampled pairs. Note that we explored the theoretical property of SGD in Appendix A.

4. Simulation

4.1. Setting

To evaluate the finite sample performance of the proposed DeepR-AFT we conduct extensive simulation experiments. We assume that failure times T_i s given covariates are generated from an AFT model, $\log T_i \sim f(\mathbf{x}_i) + \epsilon_i$, $i = 1, \dots, n$. We consider three covariates, $\mathbf{x}_i = (x_{i1}, x_{i2}, x_{i3})^\top$ where $x_{i1} \sim \text{Bernoulli}(0.5)$, $x_{i2} \sim \mathcal{N}(x_{i1}/2, 1.0)$, and $x_{i3} \sim \mathcal{N}(x_{i2}/2, 1.0)$. For the functional form of the mean part, $f(\mathbf{x})$, we consider three different forms: two nonlinear and one linear relationships. Specifically, (i) a nonlinear function including an interaction term: $f(\mathbf{x}) = 2x_1 + x_2x_3 + 2x_3$, (ii) generalized additive model (GAM) type

function: $f(\mathbf{x}) = x_1 + 0.5x_2^2 + \exp(0.1x_3)$, and (iii) a purely linear function: $f(\mathbf{x}) = x_1 + 2x_2 + 2x_3$. For error distributions, we consider the following four distributions: standard normal, Gumbel, t with three degrees of freedom, and Laplace(0, 1). The error distributions are shifted and scaled to have the zero mean and unit variance. Potential censoring times, C_i s, are generated from $\tau * U$ where U is a uniform (0, 1) distribution and τ s are set to 20, 40 and 60, which results in the approximately censoring proportions of 0.42, 0.34, and 0.30, for each simulation scenario, respectively.

For each simulation setting, we generate a training and test data sets independently. For the training data set, we consider 1000, and 5000 as the sample sizes. The sample size for the test data set is set at 2000.

Computational costs of evaluating the Gehan loss are could be too heavy since it requires pair-wise comparisons. Naturally, we use an mini-batch approach, which converges to the (local) minimum of the loss function using the full data. Note that the use of this sub-sampling approach could reduce the computing order from quadratic to linear with respect to the sample size. We sub-sampled pairs from the training data. Specifically, from each non-censored time ($\Delta_i = 1$), we sample five and ten samples when the data sizes are 1000 and 5000, respectively, Then, we form pairs composed of a non-censored time and sampled times. We use this sub-sampled pair, inspired by a property of the SGD algorithm, as the training data pairs. In the setup of (iii), the linear model, we use a linear activation for this setup. Using the linear activation is very similar to linear models. However, the nodes of each layer decrease in the used DNN, having the side effect of a dimension reduction. It can give the DNN an advantage in large-dimensional data analysis. We also conducted numerical studies to observe this side effect more in detail in Section 4.4.

We then input covariates in the test dataset to calculate predicted failure times. To compare the performances of the proposed DeepR-AFT, we also consider existing estimators based on parametric and semi-parametric AFT models. For the parametric AFT model (PAFT), the error distribution is assumed to follow a normal distribution with a constant variance. For the semiparametric AFT model (SAFT), the error distribution is left unspecified.

As measures for assessing prediction performances, we consider the following two measures: Mean Squared Error (MSE) and Concordance Index (C-index). An MSE is defined as

$$\text{MSE} = \frac{1}{n} \sum_{i=1}^n \left\{ \hat{f}(\mathbf{x}_i) - f(\mathbf{x}_i) \right\}^2. \quad (6)$$

where \hat{f} denotes an estimated f . A C-index is defined as

$$\text{C-index} = \frac{\sum_{i \neq j} \Delta_i \mathbb{I}(Y_i < Y_j) \mathbb{I}(\hat{f}(\mathbf{x}_i) < \hat{f}(\mathbf{x}_j))}{\sum_{i \neq j} \Delta_i \mathbb{I}(Y_i < Y_j)}. \quad (7)$$

The MSE is designed to capture differences in the estimated and true means in the log-transformed T , so it is a natural performance measure for the AFT model that models the mean of the log-transformed T . This measure has also been considered in assessing the prediction accuracy of AFT models (Ding and Nan, 2015; Seo and Kang, 2021). The C-index is the most commonly used measure of prediction accuracy in survival analysis. (Harrington and Fleming, 1982; Katzman et al., 2018; Kvamme et al., 2019). It is a proportion of the pairs of the predicted failure times that maintain the correct order in the observed failure times. Unlike the MSE, it is bounded between 0 and 1. The higher the better with taking 0.5 when the prediction is randomly done. In addition, it has a close relationship with the Area Under the Curve (AUC), another popular measure of prediction accuracy in survival analysis.

4.2. Estimation of various f

We first investigate the accuracy of estimation by MSE and C-index for our proposed DeepR-AFT under various forms for f . To compare the performances, we also consider PAFT and SAFT. For estimation of f under PAFT and SAFT, a linear predictor for f is considered, i.e., $f(\mathbf{x}) = \mathbf{x}^\top \boldsymbol{\beta}$ whose estimation can be done by plugging in estimates for $\boldsymbol{\beta}$. For estimation of $\boldsymbol{\beta}$, an MLE and induced smoothed rank-based estimator with the Gehan-type weight are used for PAFT and SAFT, respectively. Note that both PAFT and SAFT are not designed to address the nonlinear f . The implementation of the DeepR-AFT was done using the the `python3 keras`, and the calculations were done by the Titan-RTX GPUs. To calculate the

estimates under PAFT and SAFT, we use the `survreg` function in the `survival` package (Therneau, 2020) and `aftsrr` function in the `aftgee` package (Chiou et al., 2014), respectively, in R (R Core Team, 2021).

First, we report the simulation results for (i), $f(\mathbf{x}) = 2x_1 + x_2x_3 + 2x_3$, having an interaction. Here, we consider an interaction term between x_2 and x_3 while others are linear. To investigate the interaction effect, we consider the model having a relatively low signal of the main effects. Results are summarized in Table 1. The proposed DeepR-AFT is superior to the others in all cases in terms of MSEs and C-indices. All the MSEs under the proposed DeepR-AFT are smaller than those under the PAFT and SAFT. The reduction in the MSEs are larger for a larger sample size with the Gumbel and $t(3)$ errors whose distributions are either skewed or heavy tailed; the MSE under the proposed DeepR-AFT is approximately 0.45 times those under the PAFT and SAFT. Similar patterns can be found for the C-indices. The advantage of the proposed DeepR-AFT is that the DNN can capture the interaction effect in the mean function.

Second, Table 2 shows the result for (ii), $f(\mathbf{x}) = x_1 + 0.5x_2^2 + \exp(0.1x_3)$, a GAM type function that includes a nonlinear relationship but without any interactions. The findings are similar to those under (i). The proposed DeepR-AFT produces similar or smaller MSEs, and higher C-indices than those under the non DeepR-AFTs (PAFT and SAFT). The proposed DeepR-AFT is slightly inferior to the PAFT or SAFT in terms of the MSE with the high censoring rate ($\tau = 20$) and small data size ($n = 1000$), but it outperforms the others when increasing the sample size from $n = 1000$ to 5000. Because we use the rank-based Gehan loss built on the ranks of residuals, the gain in the C-index can be larger than that in the MSE.

Third, the simulation results for (iii), $f(\mathbf{x}) = x_1 + 2x_2 + 2x_3$, a simple linear relationship, are summarized in Table 3. For this setup, we use a linear activation function in the proposed DeepR-AFT. The results in Table 3 show that the overall performances of the non DeepR-AFTs are better than those of the proposed DeepR-AFT in MSEs, especially for the smaller sample size ($n = 1000$). The gaps in the MSEs, however, decrease as the sample size increases. Notice that DNNs are designed to capture trends that go beyond a simple linear. Consequently, when the true relationship is linear, estimated f s under the proposed DeepR-AFT tend to have a larger variability than the those designed to capture just a simple linear trend. This may explain why the MSEs under the PAFT and SAFT are smaller than those under the DeepR-AFT when the underlying mean function is linear. Meanwhile, the C-indices of the proposed DeepR-AFT are either comparable to those of the PAFT or higher. This is, again, mainly due to the nature of the Gehan-type loss function which uses the ranks of the residuals.

In summary, the proposed DeepR-AFT appears to perform better than the PAFT and SAFT when the underlying mean functions are complex with interactions or nonlinear relationships and sample sizes are large. Under the mean function with a simple linear relationship, the DeepR-AFT produces mixed results; When the MSE is considered, the proposed DeepR-AFT appears slightly inferior to the PAFT and SAFT. On the other hand, it shows comparable or better performances in terms of the C-index. In Section 4.4, we further investigate the performance of our proposed DeepR-AFT when the linear predictor is assumed for the mean part but with large-dimensional covariates with only a few affecting the mean function.

Table 1: Simulation results for $f(\mathbf{x}) = 2x_1 + x_2x_3 + 2x_3$. Larger values of τ correspond to smaller censoring rates. Four error distributions are considered: standard normal (Gaussian), Gumbel (Gumbel), Laplace (Laplace) and t with 3 degrees of freedom ($t(3)$). Results are MSEs and C-indices in parentheses averaged over 100 replicates with two sample sizes $n = 1000$ and 5000 for training data sets.

	τ	$n = 5000$			$n = 1000$		
		DeepR-AFT	PAFT	SAFT	DeepR-AFT	PAFT	SAFT
Gaussian	20	1.976 (0.897)	2.304 (0.872)	2.115 (0.873)	2.017 (0.889)	2.335 (0.873)	2.149 (0.874)
	40	1.484 (0.894)	2.159 (0.868)	1.997 (0.869)	1.587 (0.886)	2.137 (0.868)	1.978 (0.869)
	60	1.250 (0.893)	2.055 (0.867)	1.910 (0.868)	1.340 (0.885)	2.086 (0.864)	1.940 (0.867)
Gumbel	20	1.343 (0.915)	2.358 (0.880)	2.128 (0.881)	1.677 (0.908)	2.396 (0.879)	2.162 (0.880)
	40	1.124 (0.911)	2.189 (0.874)	1.994 (0.875)	1.352 (0.904)	2.195 (0.873)	2.002 (0.874)
	60	0.973 (0.909)	2.094 (0.872)	1.921 (0.873)	1.167 (0.901)	2.107 (0.872)	1.927 (0.872)
Laplace	20	1.790 (0.902)	2.301 (0.877)	2.129 (0.878)	1.882 (0.889)	2.326 (0.877)	2.168 (0.878)
	40	1.291 (0.898)	2.178 (0.874)	2.026 (0.875)	1.318 (0.887)	2.165 (0.874)	2.014 (0.875)
	60	1.099 (0.897)	2.077 (0.872)	1.937 (0.873)	1.286 (0.886)	2.085 (0.872)	1.942 (0.873)
$t(3)$	20	1.332 (0.910)	2.294 (0.886)	2.154 (0.887)	1.941 (0.898)	2.324 (0.885)	2.184 (0.886)
	40	1.369 (0.907)	2.154 (0.882)	2.024 (0.883)	1.694 (0.895)	2.171 (0.881)	2.029 (0.882)
	60	1.010 (0.905)	2.093 (0.881)	1.961 (0.881)	1.426 (0.893)	2.092 (0.880)	1.967 (0.881)

Table 2: Simulation results for $f(\mathbf{x}) = x_1 + 0.5x_2^2 + \exp(0.1x_3)$. Larger values of τ correspond to smaller censoring rates. Four error distributions are considered: standard normal (Gaussian), Gumbel (Gumbel), Laplace (Laplace) and t with 3 degrees of freedom ($t(3)$). Results are MSEs and C-indices in parentheses averaged over 100 replicates with two sample sizes $n = 1000$ and 5000 for training data sets.

τ		$n = 5000$			$n = 1000$		
		DeepR-AFT	PAFT	SAFT	DeepR-AFT	PAFT	SAFT
Gaussian	20	0.614 (0.731)	0.609 (0.675)	0.616 (0.675)	0.685 (0.704)	0.589 (0.676)	0.579 (0.676)
	40	0.335 (0.726)	0.610 (0.669)	0.607 (0.669)	0.413 (0.705)	0.584 (0.666)	0.576 (0.666)
	60	0.234 (0.724)	0.603 (0.666)	0.598 (0.666)	0.325 (0.704)	0.576 (0.663)	0.569 (0.663)
Gumbel	20	0.451 (0.774)	0.585 (0.696)	0.578 (0.696)	0.496 (0.755)	0.615 (0.694)	0.587 (0.694)
	40	0.299 (0.758)	0.594 (0.681)	0.594 (0.681)	0.340 (0.742)	0.606 (0.681)	0.588 (0.681)
	60	0.246 (0.751)	0.588 (0.680)	0.591 (0.680)	0.290 (0.738)	0.586 (0.677)	0.574 (0.677)
Laplace	20	0.530 (0.737)	0.585 (0.690)	0.589 (0.690)	0.645 (0.705)	0.595 (0.690)	0.590 (0.690)
	40	0.302 (0.737)	0.583 (0.681)	0.584 (0.681)	0.440 (0.706)	0.589 (0.682)	0.581 (0.683)
	60	0.239 (0.736)	0.577 (0.679)	0.583 (0.679)	0.379 (0.706)	0.580 (0.679)	0.572 (0.680)
$t(3)$	20	0.443 (0.747)	0.597 (0.705)	0.589 (0.704)	0.624 (0.719)	0.602 (0.702)	0.597 (0.703)
	40	0.274 (0.750)	0.592 (0.697)	0.591 (0.697)	0.427 (0.721)	0.591 (0.695)	0.583 (0.695)
	60	0.219 (0.750)	0.584 (0.694)	0.588 (0.694)	0.380 (0.722)	0.576 (0.694)	0.569 (0.694)

Table 3: Simulation results for $f(\mathbf{x}) = x_1 + 2x_2 + 2x_3$. Larger values of τ correspond to smaller censoring rates. Four error distributions are considered: standard normal (Gaussian), Gumbel (Gumbel), Laplace (Laplace) and t with 3 degrees of freedom ($t(3)$). Results are MSEs and C-indices in parentheses averaged over 100 replicates with two sample sizes $n = 1000$ and 5000 for training data sets.

τ		$n = 5000$			$n = 1000$		
		DeepR-AFT	PAFT	SAFT	DeepR-AFT	PAFT	SAFT
Gaussian	20	0.038 (0.937)	0.002 (0.937)	0.002 (0.918)	0.115 (0.936)	0.008 (0.937)	0.009 (0.918)
	40	0.043 (0.933)	0.002 (0.933)	0.002 (0.919)	0.095 (0.932)	0.007 (0.933)	0.007 (0.919)
	60	0.042 (0.931)	0.002 (0.931)	0.002 (0.919)	0.096 (0.930)	0.007 (0.931)	0.007 (0.919)
Gumbel	20	0.148 (0.951)	0.002 (0.937)	0.001 (0.919)	0.987 (0.950)	0.008 (0.936)	0.007 (0.918)
	40	0.115 (0.947)	0.001 (0.932)	0.001 (0.918)	0.897 (0.947)	0.007 (0.932)	0.006 (0.918)
	60	0.146 (0.945)	0.001 (0.931)	0.001 (0.919)	0.585 (0.945)	0.006 (0.930)	0.005 (0.918)
Laplace	20	0.044 (0.941)	0.002 (0.937)	0.002 (0.919)	0.184 (0.940)	0.008 (0.936)	0.006 (0.918)
	40	0.040 (0.937)	0.002 (0.933)	0.001 (0.918)	0.166 (0.936)	0.007 (0.932)	0.005 (0.918)
	60	0.045 (0.935)	0.002 (0.931)	0.001 (0.919)	0.136 (0.934)	0.007 (0.931)	0.005 (0.919)
$t(3)$	20	0.104 (0.947)	0.002 (0.936)	0.001 (0.919)	0.343 (0.947)	0.009 (0.936)	0.006 (0.919)
	40	0.102 (0.944)	0.002 (0.932)	0.001 (0.918)	0.308 (0.944)	0.011 (0.932)	0.004 (0.918)
	60	0.102 (0.942)	0.002 (0.931)	0.001 (0.919)	0.257 (0.942)	0.007 (0.931)	0.005 (0.919)

4.3. Simulation for biases and variance

In this subsection, we further investigate the performance of the proposed DeepR-AFT in the point view of the bias and variance trade-off. Since an MSE can be decomposed into biases and variances, we evaluate the proportion of the bias and variance in each MSE. To this end, we generate test sets in a different way while generating training sets in the same way as in Section 4.2; Data are generated under a fixed $\mathbf{x} = (x_1, x_2, x_3)^\top$, which leads to a fixed $f(\mathbf{x})$. In this way, an MSE can be decomposed into a squared biases $\{E[\hat{f}(\mathbf{x})] - f(\mathbf{x})\}^2$ and the variance $\text{Var}(\hat{f}(\mathbf{x}))$. The generation of test sets can be summarized as follows:

1. Generate a $\mathbf{x}_i = (x_{i1}, x_{i2}, x_{i3})^\top$.
2. Generate 100 ($j = 1, \dots, 100$) T_{ij} s and C_{ij} s at the fixed \mathbf{x}_i
3. Obtain 100 \hat{f}_{ij} s for DeepR-AFT, PAFT and SAFT, and calculate an MSE, squared bias and variance
4. Repeat $i = 1$ to 2000.

Among the setups in Section 4.2, we consider $\tau = 40$, training sample size of 3000, and Gaussian error distribution. The squared bias and variance are measured for a test data set of size 2000, and the average and standard deviation are calculated over 100 samples. The results are shown in Table 4.

The results show that, for the GAM type and nonlinear cases including an interaction, biases of the SAFT and PAFT are larger than those of the DeepR-AFT. In the linear case, however, the relationship is reversed; the DeepR-AFT has a larger bias. DeepR-AFT shows relatively higher variances with respect to the squared biases, compared to nonlinear f s. Note that, for the GAM type and nonlinear cases, the proportion of the squared biases is dominant in a given MSE, with at least 5 times being larger than the variance.

In the GAM type and nonlinear cases, considering larger discrepancies in biases and smaller MSEs of the DeepR-AFT, the variances have little effects in the performances of the DeepR-AFT, implying the DeepR-AFT can address the bias well with small variance. In the linear relationship situation, as expected, the SAFT and PAFT show very low squared biases with higher values of variances. The DeepR-AFT shows similar magnitudes of squared biases and variances, both are larger than those of the PAFT and SAFT, indicating an inferior performance to the SAFT and PAFT.

To further investigate the behavior of biases, we draw plots of the true $f(\mathbf{x})$ s versus averaged predicted $f(\mathbf{x})$ s (in red) overlaid by the bars representing the 0.025 and 0.975 quantiles (in black) based on 100 replications. When the curve in each plot is closer to the unit slope line, it implies small biases. The plots show that, for the linear case, all three methods seem to be virtually unbiased. For the other two cases, some biases are observed. The PAFT and SAFT show highly wiggly patterns in both cases compared to those of the DeepR-AFT. For the GAM type, the averaged predicted $f(\mathbf{x})$ s form a pattern farther away from the unit slope line, which also explains the large degrading in C-indices in Table 2. In summary, with respect to MSEs, the DeepR-AFT provides better estimators for the mean functions with complex nonlinear relationships while its performance is not necessarily as good as those of the PAFT and SAFT when a simple linear relationship is postulated.

Model	Measure	Linear	GAM-type	Nonlinear
DeepR-AFT	Bias ²	0.0306 (0.0439)	0.2906 (0.7328)	1.4929 (5.9032)
	Var	0.0312 (0.0369)	0.0588 (0.0374)	0.1278 (0.1629)
SAFT	Bias ²	< 0.0001 (< 0.0001)	0.5687 (2.0995)	2.0783 (6.8243)
	Var	0.0025 (0.0015)	0.0022 (0.0013)	0.0041 (0.0027)
PAFT	Bias ²	< 0.0001 (< 0.0001)	0.5749 (2.0867)	2.2368 (7.3661)
	Var	0.0024 (0.0015)	0.0021 (0.0012)	0.0044 (0.0031)

Table 4: Squared Biases and Variances for various f s. Results are squared biases (Bias²) and variances (Var) averaged with the sample size $n = 2000$ for test data sets with their empirical variances in parentheses.

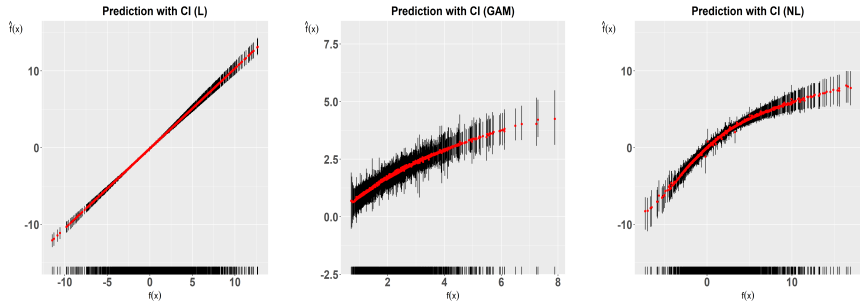


Figure 2: Left to right: plots of predicted means based on the proposed DeepR-AFT versus true means for the linear (L), GAM-type (GAM), and nonlinear including an interaction (NL) where the upper and lower bars denote the 0.025 and 0.975 quantiles, respectively.

4.4. Large dimensional covariates

In this subsection, we evaluate the performances of DeepR-AFT with large dimensional covariates when f is linear. As shown in Section 4.2, in terms of MSEs, the DeepR-AFT does not seem to perform better than the conventional AFT estimators. However, it has been reported that the DNN generally performs better in larger dimensional data (Hao et al., 2021). Therefore, we examine another simulation study

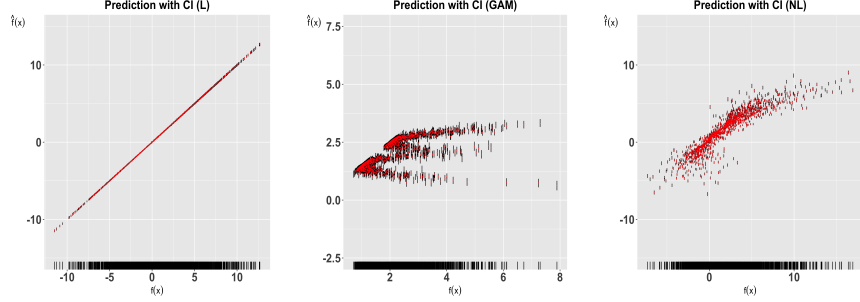


Figure 3: Left to right: plots of predicted means based on the semiparametric AFT model versus true means for the linear (L), GAM-type (GAM), and nonlinear including an interaction (NL) where the upper and lower bars denote the 0.025 and 0.975 quantiles, respectively.

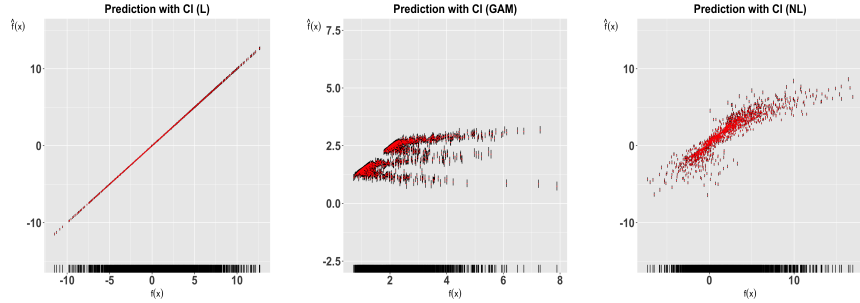


Figure 4: Left to right: plots of predicted means based on the parametric AFT model versus true means for the linear (L), GAM-type (GAM), and nonlinear including an interaction (NL) where the upper and lower bars denote the 0.025 and 0.975 quantiles, respectively.

concerning a larger dimensional data. Specifically, we consider the setting with the linear predictor for f , i.e., $f(\mathbf{x}) = x_1 + 2x_2 + 2x_3$ with the training sample size of 1000 and a Gaussian error. We add K -dimensional covariates with no effects generated from the standard normal distributions. The corresponding f is then $f(\mathbf{x}) = x_1 + 2x_2 + 2x_3 + \sum_{k=4}^K \beta_k x_k$ where $\beta_k = 0, \dots, K$. For the number of added covariates, we consider 0 to 1000.

Figure 5 shows the C-indices and $\log(MSE)$ s evaluated in the test dataset of size 2000 for different numbers of added covariates. As shown in Figure 5, the C-index for each model decreases as the dimensions become larger. The rate of decreasing for the DeepR-AFT is the smallest; Adding non-significant covariates does not seem to have substantial effects in terms of the C-index. The DeepR-AFT still work well when the dimension of the non-significant additive covariates is 1000 with the corresponding C-index being 0.88. This is not the case, however, for the conventional AFT estimators under the PAFT and SAFT. Note that we only report the results for the PAFT and SAFT when the numbers of the added non-significant covariates are 700 or less and 300 or less, respectively, because of too large computational burdens. The PAFT shows a drastic decrease when the dimensions are over 500. The SAFT shows a similar pattern to that of the DeepR-AFT with dimensions being 300 or less but no results are available beyond this. This also shows limitations of the conventional AFT models in the computational aspects. The overall results for the MSEs are comparable to those for the C-indices, with slightly larger values for the DeepR-AFT than for the PAFT when the same number of additional non-significant covariates is considered. In this case, the MSEs of PAFT and AFT get larger than those of the DeepR-AFT when the dimensions get larger. In summary, when the dimensions of the added covariates are relatively small, the DeepR-AFT can preserve the order of the mean failure times in close proximity to their true order, despite the MSEs being generally higher. DeepR-AFT is superior to the others in terms of MSE, C-index, and computational aspects in larger dimensions. This implies that, despite the application of linear activation, DNNs are still capable of extracting useful information from large dimensional inputs.

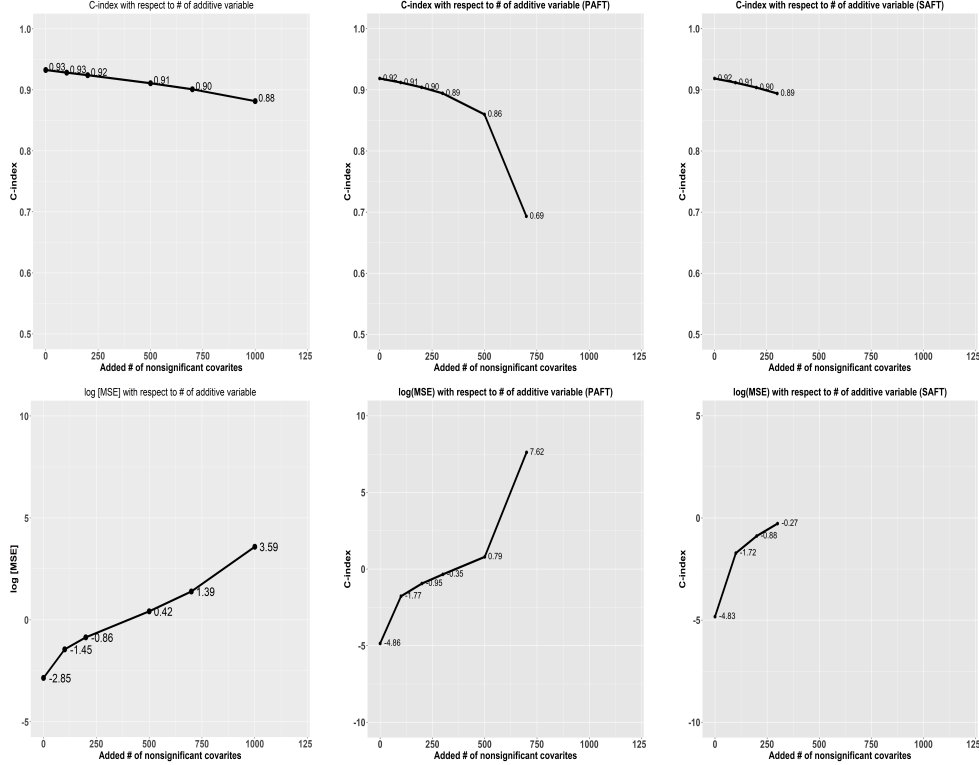


Figure 5: Top to bottom: Plots of C-indices and log(MSE)s for different numbers of added non-significant covariates. Left to right: models considered - DeepR-AFT, PAFT, and SAFT.

5. Real data analysis

5.1. Data descriptions

In this section, we illustrate an application of our proposed DeepR-AFT by analyzing the two datasets, referred to as *FL-CHAIN* and *NWTG*. The *FL-CHAIN* dataset (Dispenzieri et al., 2012; Kyle et al., 2006) is from a study intended to evaluate the relationship between serum free light chain (FLC) and mortality risk. The dataset is composed of 7874 subjects, an age- and gender-stratified random sample of the original 15759 subjects. Death is the event of interest, while survival time is defined as the number of days between enrolment and death. Covariates in the dataset include age at baseline (in years), sex (female or male), the calendar year that a blood sample was obtained, kappa portion of serum FLC, lambda portion of serum FLC, FLC group indicator, serum creatinine level, and a binary indicator for the history of a diagnosis of monoclonal gammopathy. After eliminating the samples of individuals with 0 survival times and missing serum creatinine values, the censoring rate for the remaining 6521 participants is 70%.

The second dataset is the National Wilms' Tumor Group (NWTG) study data (D'angio et al., 1989; Green et al., 1998). Wilms' tumor is a type of kidney cancer that primarily affects children. The dataset consists of 4028 Wilms' tumor patients who participated in NWTG's two waves of clinical trials. Survival time is defined as the time from diagnosis to a relapse of the tumor. Survival times are censored if no relapse is recorded by the end of the study. The number of relapses observed is 571 with the corresponding censoring rate of 86%. Covariates include tumor histology obtained from the NWTG pathology center (UH for unfavorable histology and FH for favorable histology) and from each participating institution (UH and FH), cancer stage (I - IV), age at diagnosis (in years), and indicator for study groups (3rd wave or 4th wave). Both datasets are publicly available; The *FL-CHAIN* and *NWTG* datasets are accessible through the R packages `survival` (Therneau, 2020) and `addhazard` (Hu et al., 2017).

Model	FL-CHAIN	NWTG
DeepR-AFT	0.798	0.672
PAFT	0.796	0.659
SAFT	0.797	0.660

Table 5: The C-indices for the two real datasets: *FL-Chain* and *NWTG*.

5.2. Analysis

To implement our proposed DeepR-AFT, we employ DNNs whose architectures have nine layers. There are 128, 64, and 32 nodes for the first five layers, the following two layers, and the last two layers, respectively. Here, the ReLU activation functions are used for all layers except the final layer, which has a linear activation function connecting it to the loss function. To adequately address the real datasets, we use a more complex architecture than that used in the simulation studies. Details, including the hyperparameter tuning, are provided in Appendix B. We randomly split each dataset into the training and test datasets, similar to what is done in the simulation studies. Two-thirds of each dataset is assigned to training data, while the remaining third is assigned to test data. The performance of prediction is measured by the C-index, evaluated in the test data. The results in comparison with the PAFT and SAFT are demonstrated in Table 5.

The results show that the proposed DeepR-AFT performs better on both datasets. The increase of the C-index in the *NWTG* dataset is noticeably larger while the C-indices are comparable in the *FL-CHAIN* dataset. It implies that a strong nonlinear relationship between the covariates considered and failure times could be present in the *NWTG* dataset, whereas the nonlinear relationship is weak in the *FL-CHAIN* dataset.

6. Discussion

We studied AFT models combined with DNNs. Extensive simulation experiments and application to real datasets demonstrate that DNNs can handle complex nonlinear-nonparametric AFT models effectively. In achieving the gain of DNNs, sub-sampling loss with SGD is an effective tool. The DeepR-AFT can achieve a higher C-index in a linear mean model, although the MSE is not superior to that of conventional AFT models. Nonlinear mean AFT models exhibit the gains of DeepR-AFT, as measured by the C-index and MSE. The applications to real datasets show that the non-linear modeling can be required to real datasets since the nonlinear modeling has the higher C-index.

Additionally, the simulations with large dimensional covariates demonstrate that the DeepR-AFT can extract useful information for prediction, despite the large number of noisy covariates. Regarding the algorithm, a more automated algorithm for the learning rate and others, as well as the finding the more optimal sub-sampling size could be future research directions.

Clustered failure time data are frequently encountered in biomedical studies. Due to the correlated nature of clustered failure times, our proposed DNN methods based on the independence assumption cannot be directly applied. The Gehan loss we considered could be extended to accommodate clustered failure time data. The Gehan loss based on a marginal model approach with the working independence assumption (Jin et al., 2006) is a promising candidate as the loss function. Implementing DNN and a more optimal sub-sampling procedure accounting for the clustered nature increases complexity, which is a natural direction for future research.

Appendix A. Theoretical Property of SGD in DeepR-AFT.

For simplicity, we let f, x_t be a loss function and its argument such as parameters. The SGD algorithm updates the x_{t+1} as follows:

$$x_{t+1} = x_t - \alpha \nabla f_t(x_t), \quad t = 0, \dots, T,$$

where α is the learning rate and $\nabla f_t(x_t)$ is the mean of gradient evaluated in the t -th mini-batch samples. Here f is an object function such as the cross entropy and Gehan loss function.

Theoretical properties of SGD is surveyed by Bertsekas et al. (2011), and it is known that

$$\mathbb{E}\|x_T - x^*\|^2 \leq (1 - 2\mu\alpha)^\top \|x_0 - x^*\|^2 + \frac{\alpha\sigma^2}{2\mu}$$

where $2\mu\alpha < 1$, and f is strong convex, satisfying the following inequality:

$$f(y) \geq f(x) + f'(y)^\top (y - x) + \frac{\mu}{2}\|y - x\|^2.$$

Here, x^* is the minimizer of the object function f , and σ^2 is the (sampling) variance. Therefore, an application of a diminishing learning rate provides that the SGD can achieve x^* when f is strong convex.

In the DeepR-AFT, Gehan loss given the last layer is convex (Jin et al., 2006) similar to the cross entropy loss. However, the optimization of DeepR-AFT is nonconvex due to the many layers before the last loss function. The theoretical validation with a restriction to a convex function is usual and important to understand the property of the SGD.

Appendix B. Supplementary Material: DNN learning setups

For all simulations, we use the SGD optimizers in keras with decay rate 0.00001, momentum 0.90, and nesterov. Batch size and epochs are 50 and 500 respectively. Learning rates depend on the sample sizes and error distributions, summarized in Table 6. In addition, hyperparameters for regularization of weights and

Sample size	Error distribution	Leaning rate
1000/3000	Gaussian/Laplace/ $t(3)$	0.0003
5000	Gaussian/Laplace/ $t(3)$	0.0001
1000/3000	Gumbel	0.003
5000	Gumbel	0.002

Table 6: Learning rates of DNN for all setups.

activities are set to 0.01 for all cases.

For the *FL-Chain* and *NWTG* datasets, we used the Adam optimizers with learning rates 0.00001 and 0.00002 with batch sizes 2 and 4, respectively. Commonly for these two datasets, we used 125 epochs and 400 samples randomly selected for each non-censoring data point for the sub-sampling from all pairs of Gehan loss. Also, all continuous variables are normalized, having the zero mean and unit variance. Considering larger sizes of sub-samples than those in the simulation studies are due to more complex nature of real datasets.

Acknowledgement

Conflict of interest

The authors declare that they have no conflict of interest.

References

- D. R. Cox, Regression models and life-tables (with discussion), *Journal of the Royal Statistical Society, Series B, Methodological* 34 (1972) 187–220.
- R. L. Prentice, Linear rank tests with right censored data (Corr: V70 p304), *Biometrika* 65 (1978) 167–180.
- Z. Jin, D. Y. Lin, L. J. Wei, Z. Ying, Rank-based inference for the accelerated failure time model, *Biometrika* 90 (2003) 341–353.
- Z. Jin, D. Y. Lin, Z. Ying, Rank regression analysis of multivariate failure time data based on marginal linear models, *Scandinavian Journal of Statistics* 33 (2006) 1–23.

- L. M. Johnson, R. L. Strawderman, Induced smoothing for the semiparametric accelerated failure time model: Asymptotics and extensions to clustered data, *Biometrika* 96 (2009) 577–590.
- J. Buckley, I. James, Linear regression with censored data, *Biometrika* 66 (1979) 429–436.
- W. Stute, Consistent estimation under random censorship when covariables are present, *Journal of Multivariate Analysis* 45 (1993) 89–103.
- Z. Jin, D. Y. Lin, Z. Ying, On least-squares regression with censored data, *Biometrika* 93 (2006) 147–161.
- A. A. Tsiatis, Estimating regression parameters using linear rank tests for censored data, *The Annals of Statistics* 18 (1990) 354–372.
- Z. Ying, A large sample study of rank estimation for censored regression data, *The Annals of Statistics* 21 (1993) 76–99.
- M. Fygenon, Y. Ritov, Monotone estimating equations for censored data, *The Annals of Statistics* 22 (1994) 732–746.
- T. M. Therneau, A Package for Survival Analysis in R, 2020. URL: <https://CRAN.R-project.org/package=survival>, r package version 3.1-11.
- S. H. Chiou, S. Kang, J. Yan, Fitting accelerated failure time models in routine survival analysis with R package aftgee, *Journal of Statistical Software* 61 (2014) 1–23. URL: <https://www.jstatsoft.org/v61/i11/>.
- C. Leng, S. Ma, Accelerated failure time models with nonlinear covariates effects, *Australian & New Zealand Journal of Statistics* 49 (2007) 155–172.
- J. Z. Huang, C. Kooperberg, C. J. Stone, Y. K. Truong, Functional anova modeling for proportional hazards regression, *Annals of Statistics* (2000) 961–999.
- J. L. Katzman, U. Shaham, A. Cloninger, J. Bates, T. Jiang, Y. Kluger, DeepSurv: personalized treatment recommender system using a cox proportional hazards deep neural network, *BMC medical research methodology* 18 (2018) 1–12.
- H. Kvamme, Ø. Borgan, I. Scheel, Time-to-event prediction with neural networks and cox regression, *arXiv preprint arXiv:1907.00825* (2019).
- Z. He, Deep learning in image classification: A survey report, in: *2020 2nd International Conference on Information Technology and Computer Application (ITCA)*, IEEE, 2020, pp. 174–177.
- A. Chattopadhyay, P. Hassanzadeh, S. Pasha, Predicting clustered weather patterns: A test case for applications of convolutional neural networks to spatio-temporal climate data, *Scientific reports* 10 (2020) 1–13.
- A. S. Lundervold, A. Lundervold, An overview of deep learning in medical imaging focusing on mri, *Zeitschrift für Medizinische Physik* 29 (2019) 102–127.
- C. Lee, W. Zame, J. Yoon, M. Van Der Schaar, Deephit: A deep learning approach to survival analysis with competing risks, in: *Proceedings of the AAAI conference on artificial intelligence*, volume 32(1), 2018.
- P. Chapfuwa, C. Tao, C. Li, C. Page, B. Goldstein, L. C. Duke, R. Henao, Adversarial time-to-event modeling, in: *International Conference on Machine Learning*, PMLR, 2018, pp. 735–744.
- L. Zhao, D. Feng, Deep neural networks for survival analysis using pseudo values, *IEEE Journal of Biomedical and Health Informatics* 24 (2020) 3308–3314.
- D. Rava, J. Bradic, Deephazard: neural network for time-varying risks, *arXiv preprint arXiv:2007.13218* (2020).

- Y. L. Qiu, H. Zheng, A. Devos, H. Selby, O. Gevaert, A meta-learning approach for genomic survival analysis, *Nature Communications* 11 (2020) 1–11.
- B. E. Chen, P. Norman, *deepaft: Deep learning for accelerated failure time data*, R package, 2019.
- Q. Zhong, J. W. Mueller, J.-L. Wang, Deep extended hazard models for survival analysis, *Advances in Neural Information Processing Systems* 34 (2021).
- J. P. Klein, M. L. Moeschberger, *Survival analysis: techniques for censored and truncated data*, Springer Science & Business Media, 2006.
- D. Collett, *Modelling survival data in medical research*, Chapman and Hall/CRC, 2015.
- Y. Ritov, Estimation in a linear regression model with censored data, *The Annals of Statistics* 18 (1990) 303–328.
- B. M. Brown, Y.-G. Wang, Induced smoothing for rank regression with censored survival times, *Statistics in Medicine* 26 (2007) 828–836.
- S. H. Chiou, S. Kang, J. Yan, Semiparametric accelerated failure time modeling for clustered failure times from stratified sampling, *Journal of the American Statistical Association* 110 (2015) 621–629. URL: <http://dx.doi.org/10.1080/01621459.2014.917978>. doi:10.1080/01621459.2014.917978. arXiv:<http://dx.doi.org/10.1080/01621459.2014.917978>.
- P. Ma, M. Mahoney, B. Yu, A statistical perspective on algorithmic leveraging, in: *International Conference on Machine Learning*, PMLR, 2014, pp. 91–99.
- H. Wang, R. Zhu, P. Ma, Optimal subsampling for large sample logistic regression, *Journal of the American Statistical Association* 113 (2018) 829–844.
- H. Wang, Y. Ma, Optimal subsampling for quantile regression in big data, *Biometrika* 108 (2021) 99–112.
- L. Zuo, H. Zhang, H. Wang, L. Liu, Sampling-based estimation for massive survival data with additive hazards model, *Statistics in medicine* 40 (2021) 441–450.
- N. Keret, M. Gorfine, Optimal cox regression subsampling procedure with rare events, *arXiv preprint arXiv:2012.02122* (2020).
- Y. Ding, B. Nan, Estimating mean survival time: when is it possible?, *Scandinavian Journal of Statistics* 42 (2015) 397–413.
- B. Seo, S. Kang, Accelerated failure time modeling via nonparametric mixtures, *Biometrics* (2021).
- D. P. Harrington, T. R. Fleming, A class of rank test procedures for censored survival data, *Biometrika* 69 (1982) 133–143.
- S. H. Chiou, S. Kang, J. Yan, Fitting accelerated failure time models in routine survival analysis with r package *aftgee*, *Journal of Statistical Software* 61 (2014). URL: <http://www.jstatsoft.org/v61/i11>.
- R Core Team, *R: A Language and Environment for Statistical Computing*, R Foundation for Statistical Computing, Vienna, Austria, 2021. URL: <https://www.R-project.org/>.
- L. Hao, J. Kim, S. Kwon, I. D. Ha, Deep learning-based survival analysis for high-dimensional survival data, *Mathematics* 9 (2021) 1244.
- A. Dispenzieri, J. A. Katzmann, R. A. Kyle, D. R. Larson, T. M. Therneau, C. L. Colby, R. J. Clark, G. P. Mead, S. Kumar, L. J. Melton III, et al., Use of nonclonal serum immunoglobulin free light chains to predict overall survival in the general population, in: *Mayo Clinic Proceedings*, volume 87, Elsevier, 2012, pp. 517–523.

- R. A. Kyle, T. M. Therneau, S. V. Rajkumar, D. R. Larson, M. F. Plevak, J. R. Offord, A. Dispenzieri, J. A. Katzmann, L. J. Melton III, Prevalence of monoclonal gammopathy of undetermined significance, *New England Journal of Medicine* 354 (2006) 1362–1369.
- G. J. D’angio, N. Breslow, J. B. Beckwith, A. Evans, E. Baum, A. Delorimier, D. Fernbach, E. Hrabovsky, B. Jones, P. Kelalis, et al., Treatment of wilms’ tumor. results of the third national wilms’ tumor study, *Cancer* 64 (1989) 349–360.
- D. M. Green, N. E. Breslow, J. B. Beckwith, J. Z. Finklestein, P. E. Grundy, P. Thomas, T. Kim, S. J. Shochat, G. M. Haase, M. L. Ritchey, et al., Comparison between single-dose and divided-dose administration of dactinomycin and doxorubicin for patients with wilms’ tumor: a report from the national wilms’ tumor study group., *Journal of Clinical Oncology* 16 (1998) 237–245.
- J. K. Hu, N. Breslow, G. Chan, *addhazard: Fit Additive Hazards Models for Survival Analysis*, 2017. URL: <https://CRAN.R-project.org/package=addhazard>, r package version 1.1.0.
- Z. Jin, D. Lin, Z. Ying, Rank regression analysis of multivariate failure time data based on marginal linear models, *Scandinavian Journal of Statistics* 33 (2006) 1–23.
- D. P. Bertsekas, et al., Incremental gradient, subgradient, and proximal methods for convex optimization: A survey, *Optimization for Machine Learning* 2010 (2011) 3.